Front. Struct. Civ. Eng. 2019, 13(3): 686–700
https://doi.org/10.1007/s11709-018-0506-2

RESEARCH ARTICLE

Predicting the response of continuous RC deep beams under varying levels of differential settlement

M. Z. NASER[a*], R. A. HAWILEH[b,c]

[a] *Glenn Department of Civil Engineering, Clemson University, Clemson, SC 29634, USA*
[b] *Department of Civil Engineering, American University of Sharjah, Sharjah, United Arab Emirates*
[c] *Materials Science and Engineering Research Institute, American University of Sharjah, Sharjah, United Arab Emirates*
[*] *Corresponding author. E-mail: nasermoh@msu.edu; m@mznaser.com*

ABSTRACT This paper investigates the effect of differential support settlement on shear strength and behavior of continuous reinforced concrete (RC) deep beams. A total of twenty three-dimensional nonlinear finite element models were developed taking into account various constitutive laws for concrete material in compression (crushing) and tension (cracking), steel plasticity (i.e., yielding and strain hardening), bond-slip at the concrete and steel reinforcement interface as well as unique behavior of spring-like support elements. These models are first validated by comparing numerical predictions in terms of load-deflection response, crack propagation, reaction distribution, and failure mode against that of measured experimental data reported in literature. Once the developed models were successfully validated, a parametric study was designed and performed. This parametric study examined number of critical parameters such as ratio and spacing of the longitudinal and vertical reinforcement, compressive and tensile strength of concrete, as well as degree (stiffness) and location of support stiffness to induce varying levels of differential settlement. This study also aims at presenting a numerical approach using finite element simulation, supplemented with coherent assumptions, such that engineers, practitioners, and researchers can carry out simple, but yet effective and realistic analysis of RC structural members undergoing differential settlements due to variety of load actions.

KEYWORDS concrete, continuous beams, deep beams, finite element modeling, support settlement

1 Introduction

It is quite normal for civil structures to undergo some level of settlement whether immediately post-construction due to the full (dead) weight of the structure or throughout their service life arising from ever changing occupancy and environmental conditions, etc. [1,2]. Differential settlement, on the other hand, occurs when a foundation (such as pier or footing) unequally settles due to unevenly distributing loads or when soil under foundation expands, contracts or shifts away [1–3]. This is often caused by flooding, poor drainage/compaction, icing, and vibrations from nearby construction etc. Differential settlement can result in localized structural damage (specifically cracks) that can spread throughout the structure (in walls, beams, columns), and therefore, is of great concern from safety, serviceability and stability points of view [3–5].

The adverse effects of differential settlement can be illustrated through analyzing a typical continuous (two-spanned) reinforced concrete (RC) beam that rests over three supports (namely two edges and one interior "middle" support). Such continuous beams are fairly common in civil construction and are often used as transfer beams and foundation walls. These beams are designed to carry heavy point loads, over open spaces, as to transfer them to reaction supports. As a result of this transfer mechanism, high moment and high shear develop within interior shear spans. Ashour [4] and Asin [5] had shown that the coexistence of such forces has a significant effect on crack development, propagation, and support settlement which negatively affect strength of beams. In a typical scenario, when the middle support undergoes high level of settlement as compared to edge support, a sagging moment

Article history: Received Jan 3, 2018; Accepted Mar 31, 2018

develops over this middle support. Since this additional sagging moment is unaccounted for, it can adversely stress the middle region of continuous beams, especially in poorly detailed or aging deep beams [3–7].

Such effects have been well documented in Refs. [4–10]. For example, Leonhardt and Walther [6] and Rogowsky et al. [7] reported testing of various two-span deep beams. The outcome of these experimental programs revealed that force distribution (in terms of flexural/shear capacity and support reactions) in multi-span deep RC beams were noticeably different from those in simply-supported or even in continuous shallow RC beams. For example, in simply supported beams subjected to one-point load at midspan, forces are equally transferred to end supports. On the other hand, in continuous beams, forces may not be equally transferred to end and middle supports as force distribution depends on rigidity and shear span ratio of the beams. These tests also showed that deep beams with vertical web reinforcement exhibited improved performance (i.e., higher failure loads and ductility) when compared to similar beams without any web reinforcement. It should be noted that there exists a solid database on the response of continuous deep RC beams [11–18] carried out on beams with and without internal reinforcement [13–15], and on solid beams and those with various web opening configurations [16–18]. Still, there is an apparent lack of experimental tests on behavior of deep RC beams (as in those used in buildings) under differential settlement, probably since bulk of published work was carried out to investigate differential settlement of oil tank structures, chimneys, and historical structures [19,20].

Following the aforementioned trend, the open literature also lacks numerical studies investigating behavior of multi-spanned deep RC beams undergoing differential settlement levels [8,21]. Of the few numerical studies carried out is the one conducted by Zhang et al. [8]. In this study, the authors numerically investigated the effect of support settlement on structural response of long-span suspension bridge using the finite element (FE) software, ANSYS. These authors noted that support settlement affected both strain distribution and vertical displacements as well as cable slippage of the bridge deck. Another study was carried out by Lin et al. [22] who developed a three-dimensional (3D) FE model to perform structural and pushover analyses on high-rise building subjected to varying levels of differential settlements. In Ref. [22], the authors reported that it is possible for a building to continue to behave elastically even after undergoing differential settlement of 25 mm, beyond which significant inelastic response can develop in lower floors which jeopardizes stability of buildings.

Due to the lack of experimental and numerical studies, the adverse effects of support settlement in continuous deep RC beams is not fully understood. Thus, this paper aims at numerically investigating the effect of support differential settlement on shear strength and structural behavior of two-span continuous deep RC beams. This study presents a numerical approach to aid engineers, designers, and researchers in carrying out simple and realistic analysis of RC structural members undergoing differential settlements due to variety of load actions. As such, twenty 3D nonlinear FE models were developed via ANSYS [23]. These models are first validated by comparing their predicted behavior in terms of load-midspan deflection response, crack propagation, reaction distribution and failure mode against that of the experimental data reported by Zhang and Tan [3]. Once these models were successfully validated, a comprehensive parametric study was carried out that examined a number of parameters such as ratio and spacing of the longitudinal and vertical reinforcement, compressive and tensile strength of concrete, as well as degree (stiffness) and location of support stiffness to induce varying levels of differential settlement.

2 Experimental details and loading setup

This section summarizes details of tested specimens and experimental tests carried out by Zhang and Tan [3] and used herein as a benchmark for developing the various FE models presented in this study.

2.1 Specimen details

Zhang and Tan [3] tested a total of six RC deep beams that have a width, depth and length of 180, 750 and 4400 mm, respectively. Both beam size and longitudinal reinforcement, in these tests, are kept the same in all beams, of which, three specimens were not reinforced with any web reinforcement, while the other three were reinforced with horizontal and vertical web reinforcement. The notation used to distinguish these beams was arranged such as "TCDB-A-B", where TCDB is an acronym for "two-span continuous deep beam". This acronym was followed by two main variables, i.e., "A" and "B" which indicate configuration of web reinforcement and beam supports, respectively. There are two types of web reinforcement configuration, "A" accompanied with number "1" to indicate that there is no web reinforcement and number "2" where both horizontal and vertical web reinforcement are present. The second character "B" also has three variations coded 1 through 3 where the first type refers to a beam tested with three rigid supports "1", the second refers to a beam tested with three elastic supports "2", and the last refers to beam with one elastic middle support and two rigid end supports "3". The variation of those parameters is shown in Fig. 1 and other details relating to the respective support conditions are reported in Ref. [3]. Details on tested beams were given in Fig. 1(a). In these beams, the aforementioned different support configurations lead to three degrees of settlement at middle and edge supports.

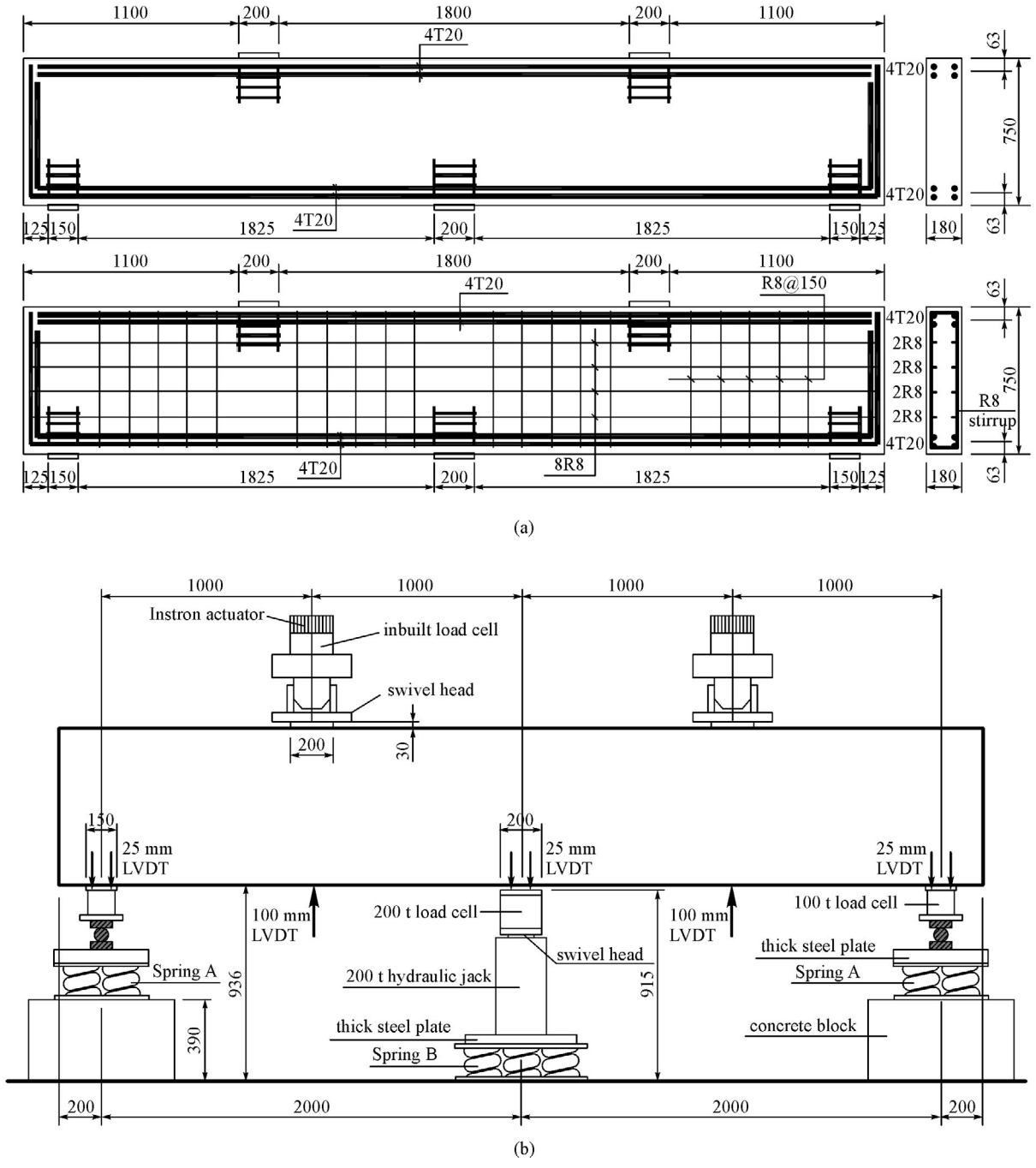

Fig. 1 Dimensions of RC deep beams and typical reinforcement layout (courtesy of Zhang and Tan [3]). (a) Details of tested specimen; (b) details of loading set-up

For example, specimen TCDB-1-2 is not provided with any web reinforcement, and tested while resting on three elastic supports (Fig. 1(b)).

Further, two types of steel reinforcement are used in the tested beams, namely, deformed high-tensile steel for main longitudinal reinforcement and plain mild-steel for web reinforcement. The RC beams are reinforced with four steel bars, arranged in two layers throughout the entire length of RC beams. The bottom longitudinal bars also have a 90° bend at their ends to anchor and provide sufficient development length. In the three beams without any web reinforcement, local steel cages were provided at points of applied vertical loading and supports to prevent premature crushing of concrete upon loading. It should be noted that a homogenous concrete mix designed to have compressive strength of 40 MPa was used in all tested beams. In order to investigate the effect of varying settlement levels, two types of springs were specially

fabricated, with nominal spring stiffness's of 68 and 101 kN/mm, respectively. These springs were either applied at end supports (of stiffness 68 kN/mm) or at end and middle support (of stiffness 101 kN/mm). Further details on tested specimens and tests can be found in Ref. [3].

2.2 Testing setup

As discussed earlier, a typical experimental set-up of a beam resting on three elastic supports is shown in Fig. 1(b). This set-up was developed to produce small differential support settlement under both end and middle supports. The set-ups for specimens with one elastic support and three rigid supports are similar to that shown in Fig. 1 but slightly modified by replacing the elastic springs with rigid concrete blocks. In all tests, two-point loads are applied at the top portion of each span using two hydraulic actuators. To record reaction forces, the authors used load cells, laid under middle and end supports. In all cases, the lengths of end and middle support were 150 and 200 mm, respectively.

Before testing of any beam specimen, an initial load of 50 kN is applied at each loading point. To ensure that both interior and edge supports are equally leveled, the middle support was first elevated using a 200-ton hydraulic actuator. Then the beam is tested through load-control mode at an increment of 20 kN until formation of cracks. Once the first flexural crack is spotted, the applied loading increment is then increased to 40 kN till the total applied load reaches around 75% of their shear capacity. At this point, both hydraulic actuators are toggled from load-control mode to displacement-control mode. Then, the test is continued in order to prevent brittle failure of the beam specimens.

3 Development of finite element model

In previous studies [24–31], the authors, among other researchers developed various FE models to predict the response of RC structural members subjected to different loadings and environmental conditions. These models varied in complexity from those developed using generic simulation environments to those implementing sophisticated features and numerical techniques. The literature review has revealed the lack of numerical models able to analyze the behavior of RC deep beams with differential settlement. Consequently, one of the objectives of this study is to develop nonlinear FE models to numerically predict the performance of continuous deep RC beams with different support settings. Due to the symmetry of the tested beams in terms of their geometrical, material, loading, and boundary conditions properties, a half beam was modeled using a FE software (ANSYS) [23]. The advantage of adopting such numerical technique lies in maintaining high solution accuracy while reducing total number of elements and nodal degrees of freedom which will result in efficient simulation and large savings of computational time. Figure 2 shows a sample of the developed 3D FE models along with the boundary conditions and loading set-up.

The symmetry boundary conditions were developed by introducing vertical restraints (i.e., rollers) at each node located in the plane of symmetry (at longitudinal direction). In order to ensure accurate simulation, the models were developed such that they share the same geometrical and material properties to that of the tested specimens presented in Ref. [3]. Further, to distinguish between the experimental beams and numerical FE models, the same acronym used in the experimental program was also followed with an added prefix "FE" to the labeling of the developed FE models.

3.1 Elements types

In this study, multiple element types were used to discretize the developed models (RC beams). For instance, the concrete material was modeled using brick "SOLID65" elements [23]. This element is capable of modeling crushing and cracking of concrete material and has 8 nodes where each node has three translational degrees of freedom (DOF). SOLID45 is another brick element and was used to simulate rigid supports and loading points [23,30]. The implementation of such modeling technique is known to prevent development of major stress concentration in concrete material, specifically at loading points and supports [25–27,31]. On the other hand, steel reinforcement (including longitudinal and web rebars) was modeled using "LINK8" elements [23]. LINK8 is capable of undergoing elastic-plastic and large deformation which typically occurs in steel reinforcement. This element is a 3D spar element defined by two nodes, each with three translational DOFs.

The use of perfect bond assumption between concrete and embedded steel interfaces continues to be a generally accepted simulation technique [32,33], however in this study, the bond-slip action between concrete surrounding horizontal and vertical steel rebars was modeled. The bond-slip between concrete and steel was simulated using "COMBIN14" spring elements [23]. COMBIN14 is a longitudinal spring-damper element (with uniaxial tension-compression capabilities) with up to three DOFs at each node [23]. It is worth noting that COMBIN14 was also used to simulated elastic supports (i.e., springs) using similar stiffness values to that documented by the manufacturer.

3.2 Material properties

The developed model comprises a number of materials similar to those used in the tested RC beams. In order to accurately simulate each material, appropriate constitutive

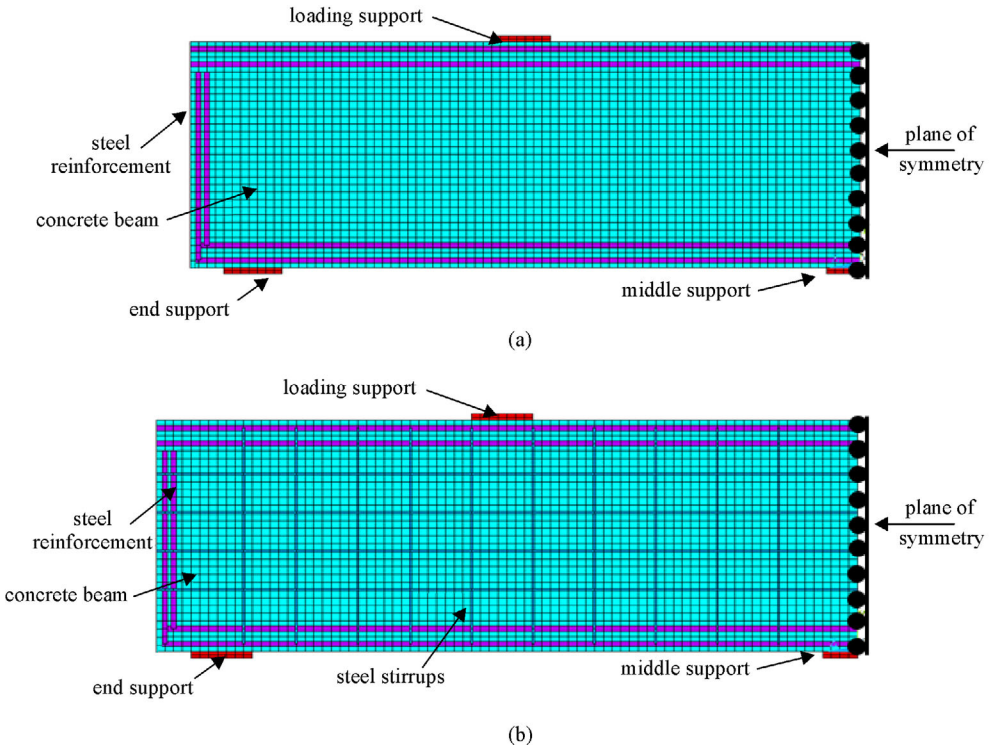

Fig. 2 Details of the developed FE model. (a) Without web reinforcement; (b) with web reinforcement

material laws were input to each of these materials. Concrete was modeled using the Williams and Warnke [34] formulation nonlinear constitutive material model implemented in ANSYS [23]. Generally, the nonlinear response of a RC structure is caused by three major factors, cracking of concrete, nonlinearity of concrete in compression, and plasticity of the reinforcement steel rebars. Up to the first crack of concrete, the behavior is linear but afterwards it becomes nonlinear. To incorporate this plastic behavior of concrete, a multi-nonlinear compressive stress-strain curve was defined. The compressive behavior of concrete is linear up to the proportional limit stress value, which is about 20%–30% of the ultimate compression stress. Beyond this stress level, the response is nonlinear (parabolic). The compressive nonlinear concrete behavior is modeled using the model derived by Hognestad et al. [35] presented in Eq. (1). The concrete material had a compressive strength of 40 MPa, a modulus of elasticity of 22 GPa, and a Poisson's ratio of 0.2. In addition,

$$f_c = f_c' \left[2\frac{\varepsilon}{\varepsilon_o} - \left(\frac{\varepsilon}{\varepsilon_o} \right)^2 \right], \quad (1)$$

where f_c is the stress in concrete (unit: MPa) corresponding to a specified strain, ε, f_c' is the concrete ultimate compressive stress (unit: MPa), ε_o is the compressive strain corresponding to f_c'.

The concrete tensile response is also modeled using a tri-linear stress-strain constitutive material model is also based on William and Wranke's model [34]. In this model, the elastic behavior of concrete in tension starts to increase linearly up to reaching concrete tensile strength (f_t), where the tensile rupture strength is taken as $0.6\sqrt{f_c'}$. When maximum tensile strength is reached, effect of stress relaxation is applied through a sudden drop of 60% in strength [23]. After this drop, tensile stress-strain linearly descends to zero stress at a strain of $6\varepsilon_t$ is followed, where ε_t is the tensile component of concrete strain corresponding to f_t.

The longitudinal and vertical steel was assumed to have an elastic-plastic stress behavior. The elastic modulus, yield strength, and Poisson's ratio of the main steel reinforcement were then assumed 202 GPa, 450 MPa and 0.3, respectively. It should be noted that a similar numerical procedure to model RC beams was followed in recent studies [26,30,31].

3.3 Bond-slip model

As discussed earlier, a bond-slip model is used to model the bond-slip action between concrete surrounding steel reinforcement. This model is based on the CEB-FIP model [34] and presented by Eq. (2). Equation (2) is derived based on first segment of the adopted CEB-FIP model [36]. The bond-slip behavior is used to calculate the stiffness of the spring COMBIN14 elements that follows the ascending segment of CEB-FIP model. Then, a horizontal plateau

is set to equal the maximum bond stress since the embedded reinforcement cannot completely debond from the surrounding concrete [36,37]. The values of the maximum bond stress and associated slip depend on rebar type and surrounding concrete materials. According to the CEB-FIP model [36], the values of $\sqrt{f_c'}$ and 0.6 mm were taken to simulate the τ_u and s_u, respectively.

$$\tau = \tau_u \left(\frac{s}{s_u}\right)^{0.4}, \quad (2)$$

where τ is the bond stress at a given slip (s) (unit: MPa), τ_u is the maximum bond stress (unit: MPa), s is the relative slip at a given shear stress (unit: mm), and s_u is the ultimate slip at τ_u (unit: mm).

The longitudinal bond-slip is modeled using COMBIN14 elements [23]. These elements require an input value for stiffness (k) and could be obtained from the secant of Eq. (2) as derived by Nie et al. [37] and presented in Eq. (3).

$$k = \frac{\pi}{s_u} p d_r N_r \tau_u \frac{L_1 + L_2}{2}, \quad (3)$$

where p is the horizontal distance between the steel reinforcement bars (unit: mm), d_r is the diameter of steel bars (unit: mm), N_r is the number of reinforcing bars, and L_1 and L_2 represent the lengths of two adjacent reinforcement elements (LINK8) (unit: mm).

3.4 Failure criteria

Failure in the carried FE simulation is attained once the solution for a load increment of 1 N does not numerically converge and/or due to excessive deflection in the model as a result of reaching plastification (i.e., cracking of concrete, yielding of steel) that exceeds plastic strain in concrete or steel materials. In this study, the force convergence criterion was selected to control convergence of simulation through a Newton-Raphson solution method. After several trials of conducting a sensitivity analysis, it was found that a convergence tolerance limit of 0.05 led to optimum solution processing time. It should be noted that typical convergence tolerance limit range in modeling concrete structures is between 0.05 to 0.20 [23–25].

3.5 Sensitivity analysis

Selection of appropriate mesh size can significantly affect predictability of an FE model [38,39]. Thus, a mesh sensitivity analysis was performed to obtain the optimum element size in this numerical study. Three different FE were developed and analyzed with mesh sizes of 25, 50, and 100 mm, respectively. The results of the mesh sensitivity analysis are provided herein. Figure 3 plots a comparison between the three different meshes, in terms of load-deflection predicted response for specimen TCDB-1-1,

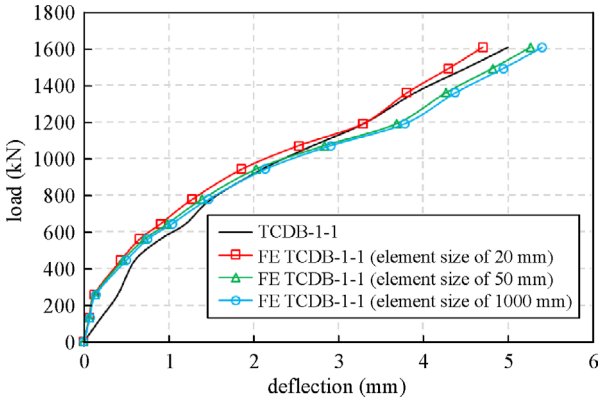

Fig. 3 Mesh sensitivity analysis

used in the mesh sensitivity analysis. It can be inferred that using a mesh size of 25 mm (as oppose to 50 or 100 mm) seems to yield the best correlation with the experimentally measured data. A unique Matlab-based methodology for carrying out a sensitivity analysis can also be followed as per the study conducted by Vu-Bac et al. [39].

4 Validation of developed FE models

The validation of the FE models was conducted through comparison of predicted and experimentally measured load-midspan deflection response reported in Zhang and Tan [3] (Fig. 4). Furthermore, Table 1 lists a detailed comparison between the FE predicted and measured experimental load-carrying capacity and corresponding maximum deflection in tested beams. It is clear from Fig. 4 and Table 1 that there is good correlation between experimentally measured and FE predicted load-midspan deflection responses. In fact, the difference between the predicted and measured load at failure was less than 3% while the difference in maximum deflection was less than 10%. It is worth noting that once shear failure occurs, a sudden and brittle drop in the load-displacement curve takes place. This drop was not presented in Fig. 4 as such drop does not provide any useful information to designers, i.e., only the maximum load at failure and associated deflection in each specimen is shown for illustration.

To further validate the FE models, the measured reaction forces in tested beams TCDB-1-1, TCDB-2-1, and TCDB-2-2 at edge and interior (middle) support was also compared against those predicted from the developed models. The comparison is plotted in Fig. 5 and it clearly shows that there is a close agreement between measured and predicted reaction forces at both edge and middle support in those beams. As typically occur in deep RC beams, reaction forces in these tested beams seem to linearly increase as a function of applied vertical loading till failure. It is worth noting that the maximum variation

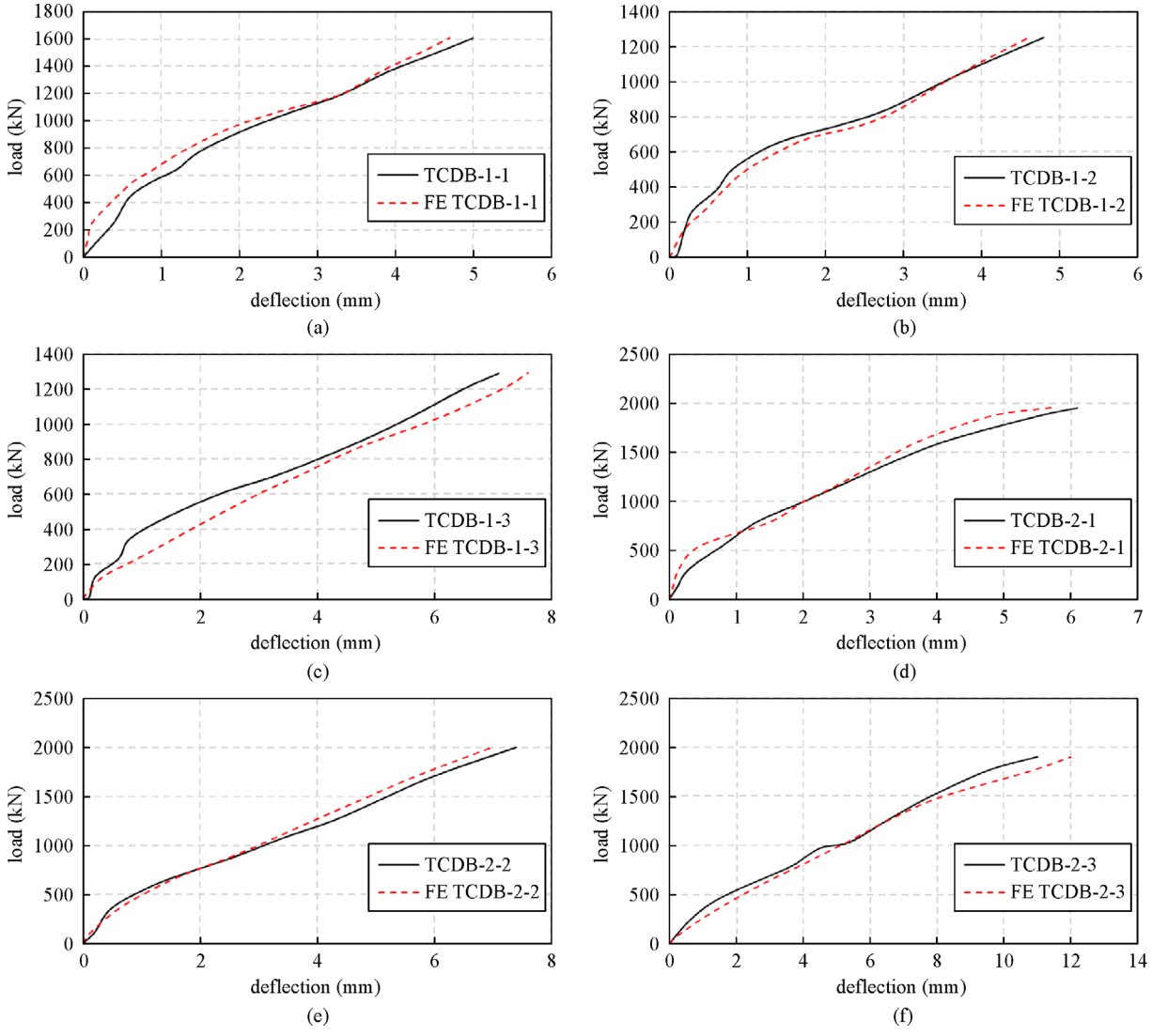

Fig. 4 Comparison between predicted and measured load-deflection response curves. Load-deflection curves for specimens (a) TCDB-1-1, (b) TCDB-1-2, (c) TCDB-1-3, (d) TCDB-2-1, (e) TCDB-2-2, and (f) TCDB-2-3

Table 1 Comparison between the FE predicted and experimental measured results

specimen	FE model	failure load (kN)		difference (%)	maximum deflection (mm)		difference (%)
		experimental	FE		experimental	FE	
TCDB-1-1	FE TCDB-1-1	1594	1608	−0.88	5.0	4.7	6.00
TCDB-1-2	FE TCDB-1-2	1274	1253	1.65	4.8	4.6	4.17
TCDB-1-3	FE TCDB-1-3	1280	1289	−0.70	7.1	7.6	−7.04
TCDB-2-1	FE TCDB-2-1	2002	1950	2.60	6.1	5.7	6.56
TCDB-2-2	FE TCDB-2-2	2002	2000	0.10	7.4	6.9	6.76
TCDB-2-3	FE TCDB-2-3	1914	1903	0.57	11.0	12.0	−9.09

between measured and predicted results was minor (of less than 5%) in all presented cases.

The observed failure modes in the tested RC beams shown in Fig. 6 are compared with those obtained from FE analysis. Figure 6 shows a comparison between the simulated and reported experimental failure modes of the tested beams TCDB-1-1, TCDB-1-2, TCDB-1-3, TCDB-2-1, TCDB-2-2, and TCDB-2-3. It is clear from the predicted and measured results that the developed models successfully managed to capture crack propagation and

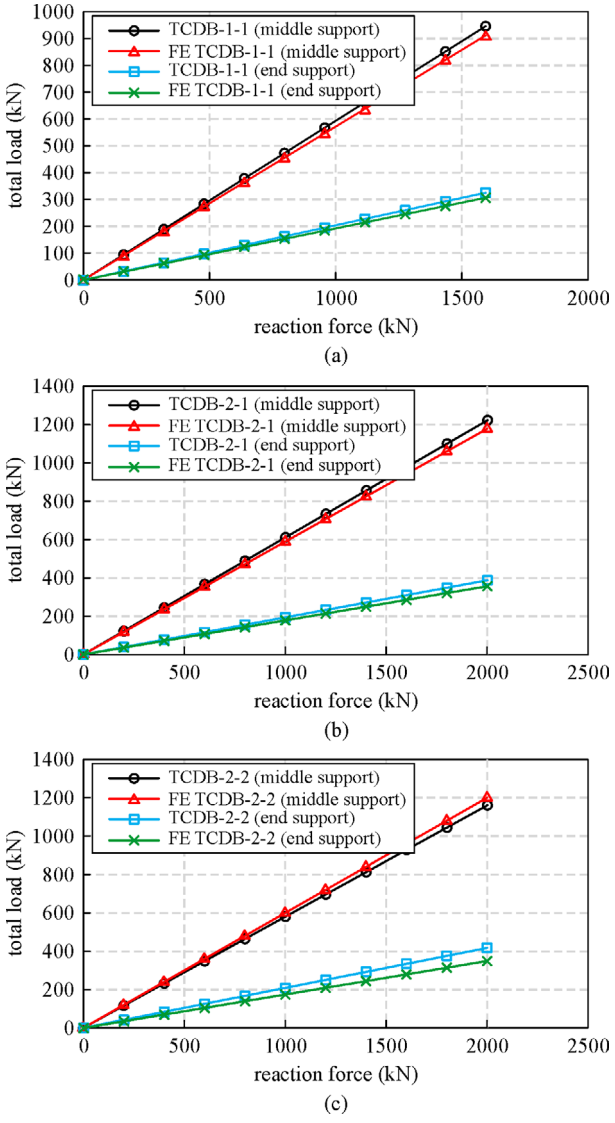

Fig. 5 Comparison between measured and predicted reaction forces in tested beams. (a) TCDB-1-1; (b) TCDB-2-1; (c) TCDB-2-2

failure mode of these beams. These cracks initiate from support region due to high concentration of shear forces and then grow at an inclined angle till reaching compression region in the loaded beam. Illustrations plotted in Fig. 6 infer that the developed FE models are well calibrated and reliable and could be extended for use as a numerical tool to investigate other aspects of continuous deep RC beams with varying support and settlement conditions.

5 Parametric study

The above validated FE models were used to carry out a parametric study in order to further investigate the effect of number of critical parameters that were not investigated in the experimental program carried out by Zhang and Tan [3] and generate results that 1) can be useful to designers and engineers, and 2) bridge knowledge gap currently present in this research area. These parameters are listed in Table 2 and include ratio and spacing of the longitudinal and vertical reinforcement, compressive and tensile strength of concrete, as well as degree (i.e., stiffness) and location of edge and interior support settlement. In order to represent a practical situation, the parametric study used RC deep beam specimen TCDB-2-2 as the main model since it had three elastic supports and adequate web steel reinforcement. It is worth noting that the capacity of elastic springs used in the experimental program were not measured nor reported. Thus, in order to avoid over-estimating structural response of developed models, the FE analysis was programed to terminate either upon reaching the maximum capacity of the spring support as measured failure load of TCDB-2-2 (2000 kN) or non-convergence of numerical solution as discussed in Section 3.4. The following sections highlight the findings of this parametric study.

5.1 Ratio of longitudinal and vertical reinforcement

In order to investigate the contribution of longitudinal and vertical reinforcement to shear (and settlement) response of continuous deep RC beams with varying elastic support conditions, four additional models were developed. These models varied steel reinforcement ratio through altering size of main (longitudinal) and vertical (stirrups) steel rebars. The sizes of steel reinforcement were either doubled “D” or reduced to half “H” of that of the size used in the actual TCDB-2-2 beam. As such, the newly developed models are referred to as FE TCDB-2-2-LD, FE TCDB-2-2-LH, FE TCDB-2-2-WD, and FE TCDB-2-2-WH, where “L” and “W” notations relate to longitudinal or web reinforcement, respectively.

The outcome of the carried-out analysis in this section is shown in Fig. 7. Figure 7(a) clearly demonstrates the noticeable effect of varying ratio of longitudinal steel reinforcement (rebar size) on response of analyzed beams. A comparison between FE TCDB-2-2-LD and TCDB-2-2 shows that specimen FE TCDB-2-2-LD achieved a similar failure load to that of the original specimen but with much lower deflection of 5.49 mm as opposed to 7.40 mm (a reduction of 25.8%). The same figure also shows that reducing size of steel reinforcement up to half of that used in beam TCDB-2-2, not only reduced shear capacity, but also caused a much larger mid-span deflection at similar load levels to that observed in TCDB-2-2. For instance, FE TCDB-2-2-LH failed at 1490 kN (which is 34% less than measured failure load in TCDB-2-2). At failure, FE TCDB-2-2-LH underwent a maximum deflection of 6.95 mm which is 23% higher than that measured in specimen TCDB-2-2 at the same load level.

Figure 7(b) also shows that the response of analyzed beams seem to be less sensitive to the increase in size of web steel reinforcement as opposed to that of the

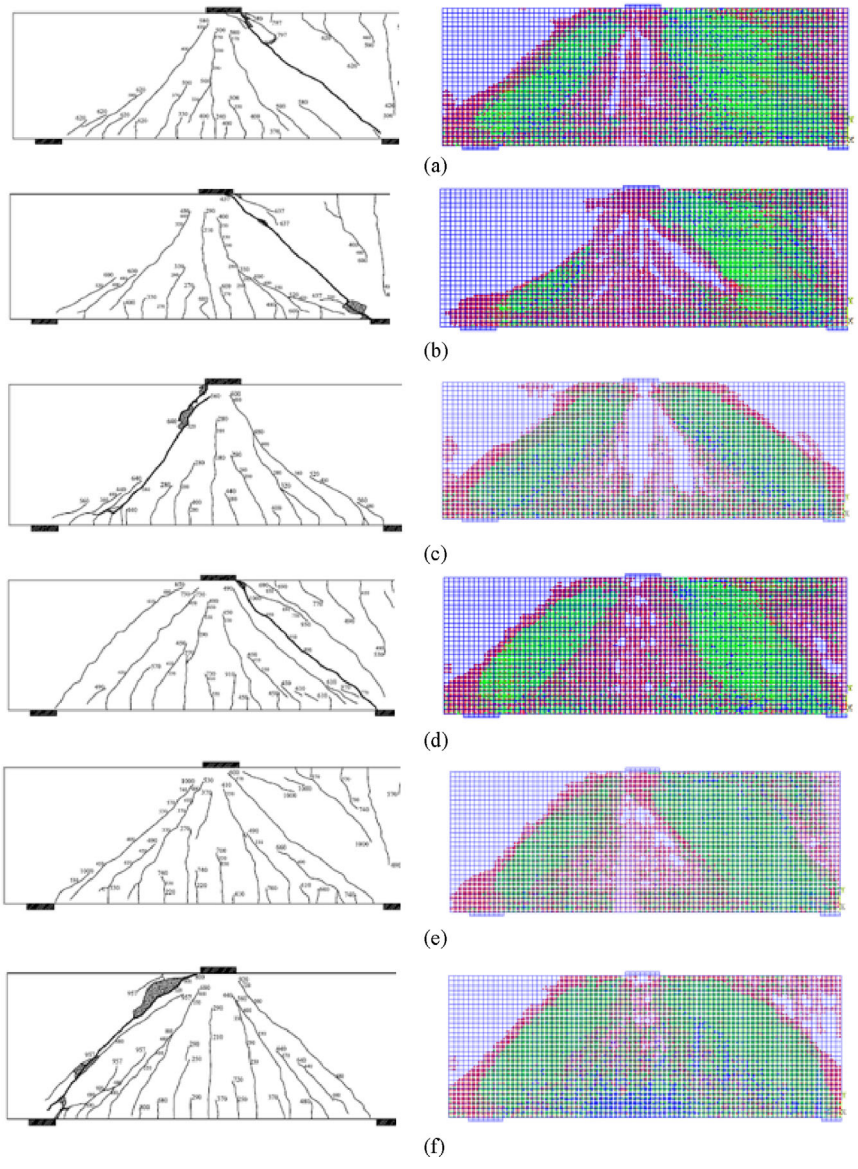

Fig. 6 Comparison between the failure modes (of one span) of the experimental and FE models (courtesy of Zhang and Tan [3]). (a) TCDB-1-1; (b) TCDB-1-2; (c) TCDB-1-3; (d) TCDB-2-1; (e) TCDB-2-2; (f) TCDB-2-3

longitudinal reinforcement. When web steel reinforcement was doubled, mid-span deflection of specimen FE TCDB-2-2-WD reduced to 6.5 mm (as compared to 7.4 mm); with a 12% reduction. This can be attributed to the fact that the originally tested specimen (TCDB-2-2) was reinforced with sufficient vertical reinforcement and any additional reinforcement would moderately improve response of beam (as opposed to the much-improved performance when longitudinal rebar size is doubled, see the response of FE TCDB-2-2-LD). The same figure also highlights the fact that this RC deep beam performs poorly with reduction in web steel ratio. For example, although beam FE TCDB-2-2-WH achieved a similar response to that of TCDB-2-2, due to the permissible redistribution effects of having elastic springs at edge and middle supports, this beam still failed under a slightly lower load of 1706 kN (17% lower than TCDB-2-2).

Finally, the effect of varying both longitudinal and vertical reinforcement on reactions at edge and middle supports was also studied as a part of this parametric study. The findings of such analysis are plotted in Fig. 8. These findings show that reactions at middle support seems to remain similar in all tested cases, while those at edge support varies according to the increase/reduction in steel reinforcement ratio. This variation at edge support can be explained by the fact that elastic spring used at this support had much lower stiffness (less stable/more prone to settle) than that at the middle support. As a result, any changes to

Table 2 List of varied parameters

parameter	beam title	varied parameter
ratio of longitudinal and vertical reinforcement	FE TCDB-2-2-LD	Steel reinforcement ratio in the longitudinal "L" direction was doubled "D".
	FE TCDB-2-2-LH	Steel reinforcement ratio in the longitudinal "L" direction was reduced in half "H".
	FE TCDB-2-2-WD	Web reinforcement ratio "W" direction was doubled "D".
	FE TCDB-2-2-WH	Web reinforcement ratio "W" direction was reduced in half "H".
arrangement of vertical reinforcement	FE TCDB-2-2-S75	Stirrups spacing "S" was reduced to 75 mm.
	FE TCDB-2-2-S300	Stirrups spacing "S" was increased to 300 mm.
compressive and tensile strength of concrete	FE TCDB-2-2-fc60	Compressive strength of concrete was increased to 60 MPa and tensile strength was increased accordingly.
	FE TCDB-2-2-fc90	Compressive strength of concrete was increased to 90 MPa and tensile strength was increased accordingly.
stiffness of edge and middle elastic support	FE TCDB-2-2-0.5K	Stiffness of supports "K" was reduced to half.
	FE TCDB-2-2-2K	Stiffness of supports "K" was doubled.
	FE TCDB-2-2-5K	Stiffness of supports "K" was scaled up by a factor of 5.
location of elastic support	FE TCDB-2-2-2KE	Stiffness of edge support "E" was doubled.
	FE TCDB-2-2-2KM	Stiffness of middle support "M" was doubled.

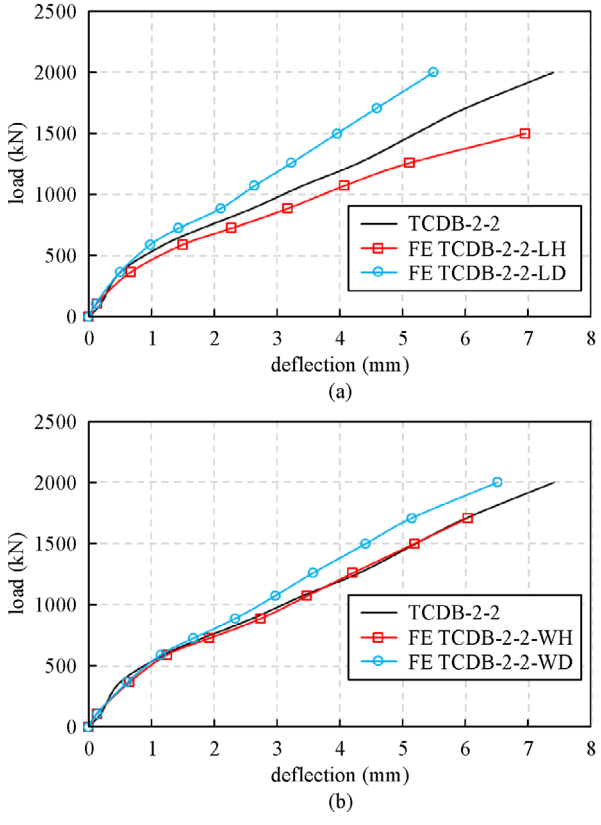

Fig. 7 Effect of ratio of (a) longitudinal and (b) vertical reinforcement on the performance of continuous deep beams

force distribution within the beam significantly affect level of reaction at edge support. In other words, the high stiffness of middle support was able to stabilize the response of simulated beams.

5.2 Arrangement of vertical reinforcement

The effect of various arrangements of web stirrups spacing "S" was also studied. For this purpose, spacing of web reinforcement was changed from 150 (as used in TCDB-2-2) to 75 and 300 mm. Thus, two model named FE TCDB-2-2-S75 and FE TCDB-2-2-S300 were developed. The load-midspan deflection response of these beams was compared against that of beam TCDB-2-2 in Fig. 9(a). This figure confirms earlier results presented in Fig. 7(b), in which the selected RC deep beams seem to have slightly better response when steel stirrups are closely spaced (at 75 mm) as opposed to that when they are spaced at 150 or 300 mm. This is due to the fact that closely spaced stirrups improve shear response and increases shear capacity of analyzed RC deep beams. The improved performance was quantified at 12% (in terms of maximum mid-span deflection at failure). Interestingly, increasing stirrups spaces (while maintaining same rebar diameter) did not seem to disrupt flexural nor shear response, probably due to the short span of these beams. It should be noted that variation in reactions at edge and middle support is plotted in Fig. 9(b) where similar findings to that discussed in Fig. 8(b) continues to hold true herein.

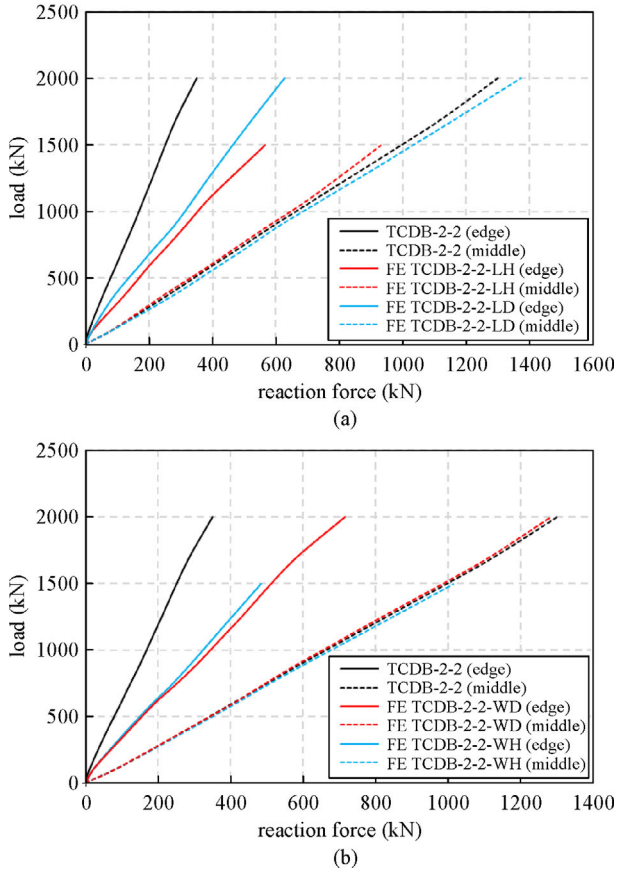

Fig. 8 Comparison between reaction forces in beams TCDB-2-2, FE TCDB-2-2-LD, FE TCDB-2-2-LH, FE TCDB-2-2-WD, and FE TCDB-2-2-WH. (a) Effect of longitudinal reinforcement; (b) effect of vertical reinforcement

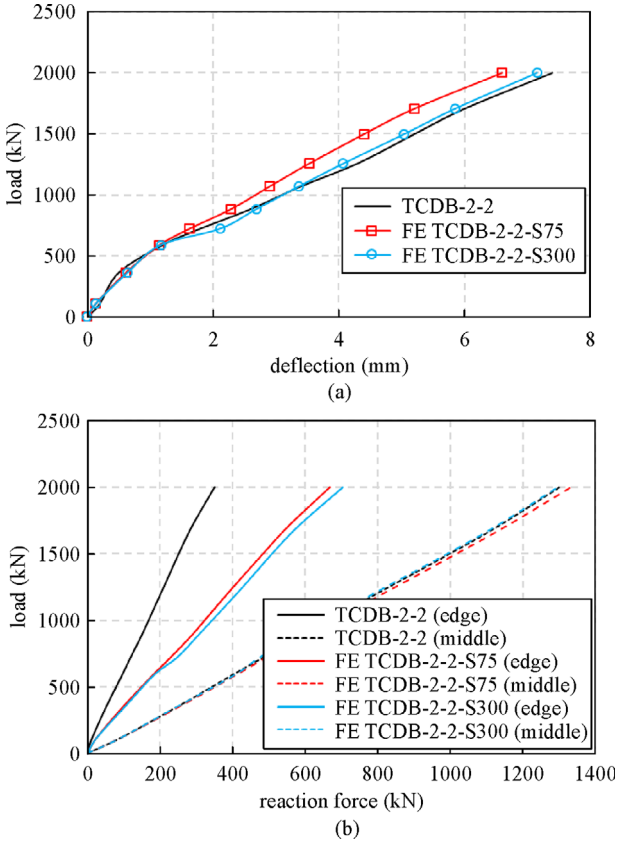

Fig. 9 Comparison between reaction forces in beams TCDB-2-2, FE TCDB-2-2-S75 and FE TCDB-2-2-S300. (a) Effect of varying stirrup spacing on load-midspan deflection response; (b) variation in reaction forces

5.3 Compressive and tensile strength of concrete

Several studies have pointed out that structural response of RC deep beams can be governed by tensile (and correspondingly compressive) strength of concrete [4–6,16]. Thus, these parameters were varied and studied in this section. For simplicity, these parameters were varied as a function of compressive strength of concrete. Since the compressive strength in the selected beam (TCDB-2-2) was 40 MPa, two different concrete compressive strengths of 60 and 90 MPa were used as input into two additionally developed FE models, named as FE TCDB-2-2-fc60 and FE TCDB-2-2-fc90, respectively. As a result of varying compressive strength of concrete, the tensile strength of concrete was also varied and taken as $0.6\sqrt{f_c'}$ as the tensile strength is a function of compressive strength of concrete.

Figure 10(a) illustrates the positive effect of using concrete material with higher compressive (and tensile) strength than that used in tested beam TCDB-2-2 through improving load-midspan deflection response curves. It is clear that in both cases, the analyzed beams achieved much lower mid-span deflection of about 17.8% and 38% than that measured in beam TCDB-2-2. In addition, the cracking load, which was predicted by the developed FE models was also improved. This improved cracking behavior can be seen at the apparent "kinks" at the end of the elastic portion of the load-deflection curves plotted in Fig. 10(a). The predicted reactions at end and middle support also agrees with such observation (specifically for edge support where initial cracks were reported to develop) are shown in Fig. 10(b).

5.4 Stiffness of edge and middle elastic support

One of the major limitations reported by Zhang and Tan [3] was the high cost of elastic supports (spring elements) used in their experimental program which prevented investigating different levels of settlement in tested beams. Such limitation can be overcame through the use of validated FE models, such as the ones developed in this study. Thus, in order to study various stiffness levels of edge and interior elastic supports, three more models were developed. These models were replicas TCDB-2-2, but varied the stiffness of spring supports used at the edge and middle support. The

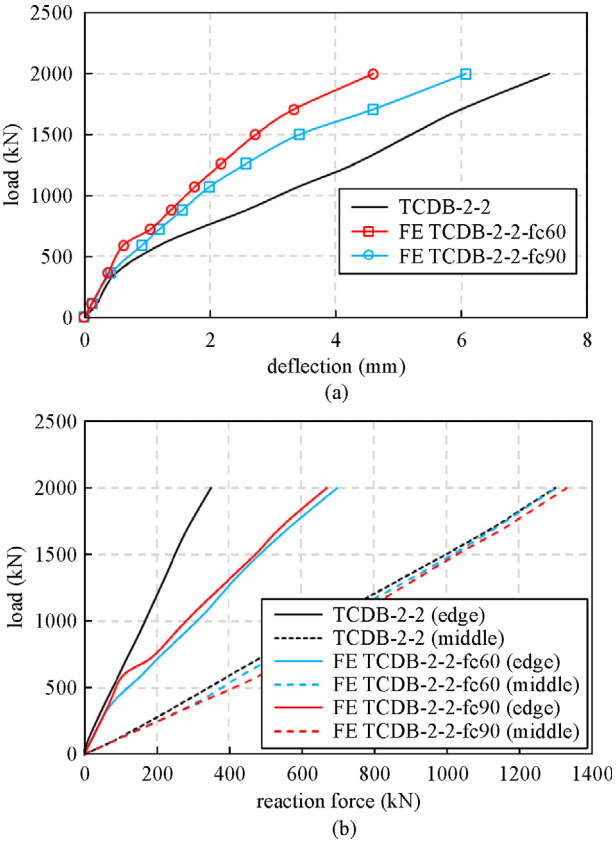

Fig. 10 Comparison between reaction forces in beams TCDB-2-2, FE TCDB-2-2-fc60 and FE TCDB-2-2-fc90. (a) Effect of varying concrete strength on load-midspan deflection response; (b) variation in reaction forces

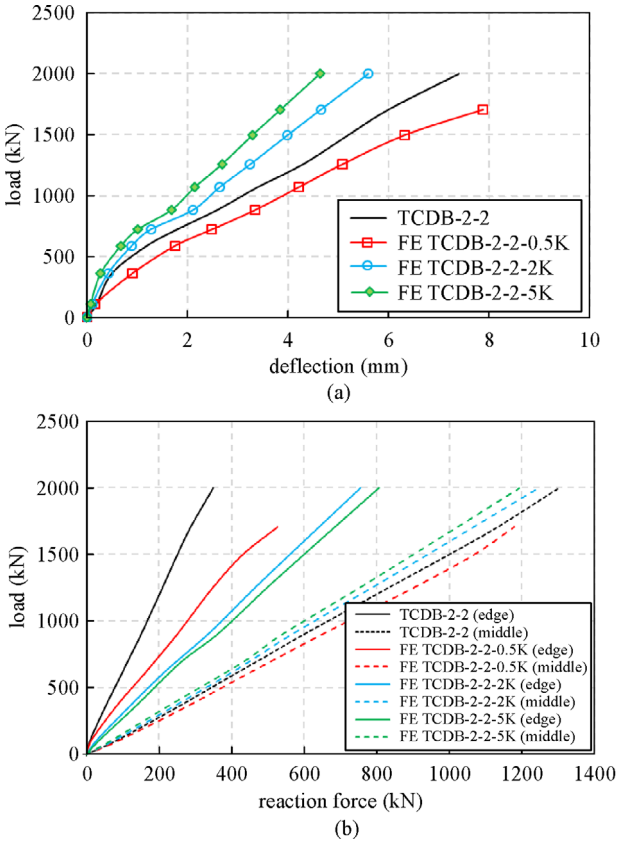

Fig. 11 Comparison between reaction forces in beams TCDB-2-2, FE TCDB-2-2-0.5K, FE TCDB-2-2-2K and FE TCDB-2-2-5K. (a) Effect of varying spring stiffness on load-midspan deflection response; (b) variation in reaction forces

variation in stiffness was scaled at 0.5, 2 and 5 times the initial stiffness of those used in the tests. As a result, the developed models were referred to as FE TCDB-2-2-0.5K, FE TCDB-2-2-2K, and FE TCDB-2-2-5K.

The outcome of this parametric study is shown in Figs. 11(a) and 11(b). As can be seen from Fig. 11, the effect of varying springs' stiffness was not linear as one would expect. In fact, plots presented in Fig. 11(a) demonstrate that the use of low stiffness (which reflects larger tendency to settle) lead to very poor performance of analyzed beam (FE TCDB-2-2-0.5K) as compared to beams with stiffer springs. This beam fails at a relatively lower load of 1660 kN, which is 17% lower than that observed in the experimental and numerical testing of beam TCDB-2-2. Further, FE TCDB-2-2-0.5K also fails with much larger settlement (mid-span deflection) of 32% larger than that of TCDB-2-2 (at the same load level). On another note, the beams with higher springs' stiffness's, i.e., FE TCDB-2-2-2K and FE TCDB-2-2-5K, achieved better performance where both failed with lower mid-span deflections of 24.3% and 37% than that of TCDB-2-2. Similar findings can also be interrupted from data plots shown in Fig. 11(b).

In order to further examine the effect of varying elastic support stiffness on response of tested beams, Fig. 12 compares crack propagation in beams TCDB-2-2, FE TCDB-2-2-0.5K, FE TCDB-2-2-2K, and FE TCDB-2-2-5K at failure. Figure 12 clearly shows the degree of damage stable beams can undergo as a function of increased settlement as compared to a beam with much lower stiffness (and instability) as in that observed in FE TCDB-2-2-0.5K. In general, beams with moderate to high support stiffness were able to undergo higher load levels and cracking before failure. Further, note the development of large compressive (crushing) stresses near top loading point in beam FE TCDB-2-2-0.5K despite the fact that this beam failed at a much lower load (1660 kN) when compared to other beams.

5.5 Location of elastic support

This section highlights the effect of varying stiffness of either edge of middle support at a given time. In other words, when edge support is scaled, the middle support remains with same stiffness to that used in the experiments. Thus, two additional models were developed in which the stiffness of edge support (E) and middle support (M) was

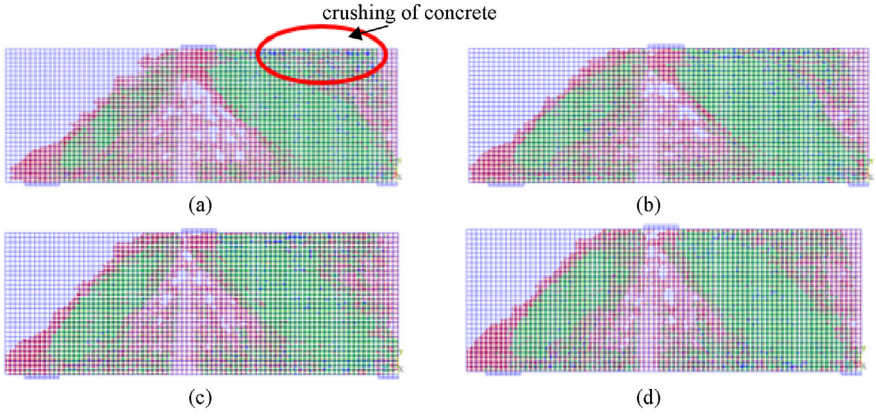

Fig. 12 Comparison of crack propagation in beams (a) FE TCDB-2-2, (b) FE TCDB-2-2-0.5K, (c) FE TCDB-2-2-2K, and (d) FE TCDB-2-2-5K at failure

varied to twice as that of their initial stiffness, i.e., nominal spring stiffness's of edge support increased to $2\times68 = 136$ kN/mm and that of middle support also increased to $2\times101 = 202$ kN/mm. The corresponding models were named as FE TCDB-2-2-2KE and FE TCDB-2-2-2KM.

The outcome of this investigation is plotted in Fig. 13 and shows that increasing stiffness of edge supports seem to have a much larger influence on the behavior of continuous RC deep beams than that of increasing stiffness of middle support. This can be attributed to the improved stability (less tendency to settle) of beam due to increasing stiffness of edge supports as compared to stability improvement arising from increasing stiffness of middle support. To further illustrate this, a closer look at Fig. 13(a) shows that FE TCDB-2-2-2KE fails at a much lower mid-span deflection (by 23.3%), while FE TCDB-2-2-2KM fails with a slightly improved mid-span deflection of 7%, but at a lower load of 1700 kN (17.2% less than TCDB-2-2). Apparently, increasing stiffness of middle to about 202/68 = 2.97 to that of edge support can facilitate significant transfer of forces to middle (stiffer) region of beam, rather than throughout the beam which ultimately over stresses middle region and lead to brittle failure of deep RC beam. This conclusion can be arrived at by examining distribution of Von-Mises stresses and developed cracks shown in FE TCDB-2-2-2KE and FE TCDB-2-2-2KM models (Figs. 13(c)–13(f)).

6 Conclusions

Twenty 3D nonlinear FE models were developed using ANSYS to investigate the response of continuous deep RC beams with varying support conditions, when subjected to gravity loading and different levels of support settlements. In addition, a newly designed parametric study consisting of fourteen models was carried out to investigate number of critical parameters such as ratio and spacing of the longitudinal and vertical reinforcement, compressive and tensile strength of concrete, as well as degree (i.e., stiffness) and location of support settlement. Based on the results of this study, the following conclusions could be drawn:

- The response of the analyzed continuous RC deep beams is sensitive to changes in longitudinal and vertical steel ratio as well as arrangement of web.
- The use of concrete with higher compressive (and subsequently) tensile strength seem to be positively improve cracking behavior, cracking response and ultimate load capacity of continuous RC deep beams.
- Significant increase of stiffness in the middle support can induced major transfer of forces to middle (stiffer) region of beam rather than throughout the beam which ultimately lead to brittle failure of RC deep beams.
- The use of FE model, when calibrated using experimental data, can overcome many of the limitations observed in full scale experiments whether related to the need for sophisticated instrumentations and/or costly equipment.

It should be noted that findings of this study infer that the developed FE models can provide unique insights into development of internal stresses and reactions, crack propagation and failure modes which can be helpful in order to accurately predict the performance of continuous RC deep beams specifically when subjected to varying levels of differential settlement. Further, these models could potentially be extended to further explore the behavior of similar RC members (shallow beams, walls, etc.) with various geometric/material configurations, support conditions, and loading conditions. While the presented FE model used ANSYS as simulation environments, it is worth noting that there also exist a number of studies specifically designed to trace the behavior of RC structures through complex and advanced simulation techniques. The readers are encouraged to visit the following studies for in-depth insights (from a fracture

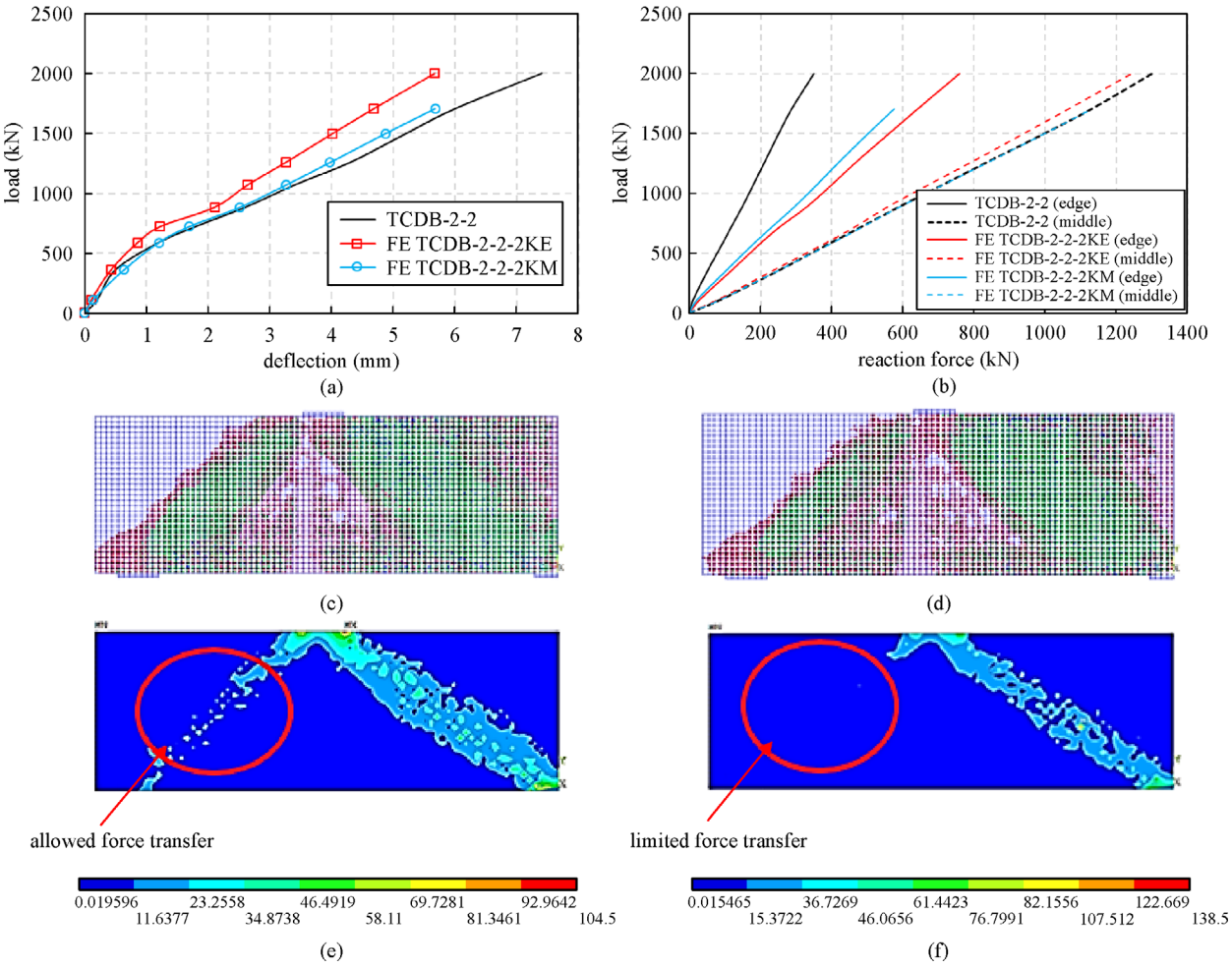

Fig. 13 Comparison in structural response between beams TCDB-2-2, FE TCDB-2-2-2KE and FE TCDB-2-2-2KM. (a) Effect of varying spring stiffness on load-midspan deflection response curves; (b) variation in reaction forces; (c) cracks in FE TCDB-2-2-2KE; (d) cracks in FE TCDB-2-2-2KM; (e) Von-Mises in FE TCDB-2-2-2KE; (f) Von-Mises in FE TCDB-2-2-2KM

mechanics point of view) into the response of RC structures under various loading effects [40–45].

Acknowledgements The authors would like to thank the editor and reviewers for their efforts in improving the state of this manuscript as well as in recommending carrying out future mathematical and numerical based studies.

References

1. Das B M, Sobhan K. Principles of Geotechnical Engineering. Boston: Cengage Learning, 2013
2. Gunaratne M. The Foundation Engineering Handbook. Boca Raton: CRC Press, 2013
3. Zhang N, Tan K H. Effects of support settlement on continuous deep beams and STM modeling. Engineering Structures, 2010, 32(2): 361–372
4. Ashour A F. Tests of reinforced concrete continuous deep beams. ACI Structural Journal, 1997, 94(1): 3–12
5. Asin M. The Behaviour of Reinforced Concrete Continuous Deep Beams. Delft: Delft University Press, 1999
6. Leonhardt F, Walther R. Deep beams. Deutscher Ausschuss Fur Stahlbeton Bulletin 178, 1970
7. Rogowsky D M, MacGregor J G, Ong S Y. Tests of reinforced concrete deep beams. Structural Engineering Report, 1983, 83(4): 614–623
8. Zhang X H, Xu Y L, Zhan S, Zhu S, Tam H W, Au H Y. Simulation of support settlement and cable slippage by using a long-span suspension bridge testbed. Structure and Infrastructure Engineering, 2017, 13(3): 401–415
9. Kim Y J, Gajan S, Saafi M. Settlement rehabilitation of a 35-year-old building: Case study integrated with analysis and implementation. Practice Periodical on Structural Design and Construction, 2011, 16(4): 215–222
10. D'Orazio T B, Duncan J M. Differential settlement in steel tanks. Journal of Geotechnical Engineering, 1987, 113(9): 967–983
11. Tan K H, Lu H Y. Shear behavior of large reinforced concrete deep beams and code comparisons. Structural Journal, 1999, 96(5): 836–846
12. Khatab M A, Ashour A F, Sheehan T, Lam D. Experimental

investigation on continuous reinforced SCC deep beams and comparisons with code provisions and models. Engineering Structures, 2017, 131: 264–274
13. Kong F K, Robins P J, Cole D F. Web reinforcement effects on deep beams. ACI Journal, 1970, 67(2): 1010–1018
14. Yang K H, Chung H S, Lee E T, Eun H C. Shear characteristics of high-strength concrete deep beams without shear reinforcements. Engineering Structures, 2003, 25(10): 1343–1352
15. Tan K H, Kong F K, Teng S, Weng L W. Effect of web reinforcement on high-strength concrete deep beams. ACI Structural Journal, 1997, 94(5): 572–582
16. Hawileh R A, El-Maaddawy T A, Naser M Z. Non-linear finite element modeling of concrete deep beams with openings strengthened with externally-bonded composites. Materials & Design, 2012, 42: 378–387
17. Yang K H, Eun H C, Chung H S. The influence of web openings on the structural behavior of reinforced high-strength concrete deep beams. Engineering Structures, 2006, 28(13): 1825–1834
18. Barney G B, Corley W G, Hanson J M, Parmelee R A. Behavior and design of prestressed concrete beams with large web openings. PCI Journal, 1977, 22(6): 32–61
19. Berardi R, Lancellotta R. Yielding from field behavior and its influence on oil tank settlements. Journal of Geotechnical and Geoenvironmental Engineering, 2002, 128(5): 404–415
20. Sykora M, Markova J, Mlcoch J, Molnar J, Presl K. Predicting service life of chimneys and cooling towers based on monitoring. In: Hordijk D, Luković M, eds. High Tech Concrete: Where Technology and Engineering Meet. Cham: Springer, 2018, 1671–1679
21. Laefer D F, Ceribasi S, Long J H, Cording E J. Predicting RC frame response to excavation-induced settlement. Journal of Geotechnical and Geoenvironmental Engineering, 2009, 135(11): 1605–1619
22. Lin L, Hanna A, Sinha A, Tirca L. High-rise building subjected to excessive settlement of its foundation: A case study. International Journal of Structural Integrity, 2017, 8(2): 210–221
23. ANSYS. ANSYS Workbench Documentation. Version 11. Canonsburg: ANSYS Inc., 2007
24. Abu-Obeidah A, Hawileh R A, Abdalla J A. Finite element analysis of strengthened RC beams in shear with aluminum plates. Computers & Structures, 2015, 147: 36–46
25. Hawileh R A, Naser M Z, Abdalla J A. Finite element simulation of reinforced concrete beams externally strengthened with short-length CFRP plates. Composites. Part B, Engineering, 2013, 45(1): 1722–1730
26. Demir A, Ozturk H, Dok G. 3D numerical modeling of RC deep beam behavior by nonlinear finite element analysis. Disaster Science and Engineering, 2016, 2(1): 13–18
27. Hawileh R A, Abdalla J A, Tanarslan M, Naser M Z. Modeling of nonlinear cyclic response of shear-deficient RC T-beams strengthened with side bonded CFRP fabric strips. Computers and Concrete, 2011, 8(2): 193–206
28. Biondini F, Vergani M. Deteriorating beam finite element for nonlinear analysis of concrete structures under corrosion. Structure and Infrastructure Engineering, 2015, 11(4): 519–532
29. Hawileh R A, Naser M Z. Thermal-stress analysis of RC beams reinforced with GFRP bars. Composites. Part B, Engineering, 2012, 43(5): 2135–2142
30. Naser M Z. Response of steel and composite beams subjected to combined shear and fire loading. Dissertation for the Doctoral Degree. East Lansing: Michigan State University, 2016
31. Naser M Z. Behaviour of RC beams strengthened with CFRP laminates under fire—A finite element simulation. Thesis for the Master's Degree. Sharjah: American University of Sharjah, 2011
32. Sakar G, Hawileh R A, Naser M Z, Abdalla J A, Tanarslan M. Nonlinear behavior of shear deficient RC beams strengthened with near surface mounted glass fiber reinforcement under cyclic loading. Materials & Design, 2014, 61: 16–25
33. Hawileh R A, Abdalla J A, Naser M Z, Tanarslan M. Finite element modeling of shear deficient RC beams strengthened with NSM CFRP rods under cyclic loading. ACI Special Publications, 2015, 301: 1–18
34. William K J, Warnke E P. Constitutive models for the triaxial behavior of concrete. Proceedings of the International Association for Bridge and Structural Engineering, 1975, 19: 1–30
35. Hognestad E, Hanson N, McHenry D. Concrete stress distribution in ultimate strength design. ACI Journal, 1955, 52(12): 455–479
36. Comite Euro-International du Beton (CEB-FIP). CEB-FIP Model Code 1990. Bulletin D'Information, 1993
37. Nie J, Fan J, Cai C. Stiffness and deflection of steel-concrete composite beams under negative bending. Journal of Structural Engineering, 2004, 130(11): 1842–1851
38. Hamdia K M, Silani M, Zhuang X, He P, Rabczuk T. Stochastic analysis of the fracture toughness of polymeric nanoparticle composites using polynomial chaos expansions. International Journal of Fracture, 2017, 206(2): 215–227
39. Vu-Bac N, Lahmer T, Zhuang X, Nguyen-Thoi T, Rabczuk T. A software framework for probabilistic sensitivity analysis for computationally expensive models. Advances in Engineering Software, 2016, 100: 19–31
40. Rabczuk T, Zi G, Bordas S, Nguyen-Xuan H. A geometrically nonlinear three-dimensional cohesive crack method for reinforced concrete structures. Engineering Fracture Mechanics, 2008, 75(16): 4740–4758
41. Rabczuk T, Akkermann J, Eibl J. A numerical model for reinforced concrete structures. International Journal of Solids and Structures, 2005, 42(5–6): 1327–1354
42. Rabczuk T, Belytschko T. Cracking particles: A simplified meshfree method for arbitrary evolving cracks. International Journal for Numerical Methods in Engineering, 2004, 61(13): 2316–2343
43. Rabczuk T, Zi G, Bordas S, Nguyen-Xuan H. A simple and robust three-dimensional cracking-particle method without enrichment. Computer Methods in Applied Mechanics and Engineering, 2010, 199(37–40): 2437–2455
44. Rabczuk T, Belytschko T. A three-dimensional large deformation meshfree method for arbitrary evolving cracks. Computer Methods in Applied Mechanics and Engineering, 2007, 196(29–30): 2777–2799
45. Rabczuk T, Belytschko T. Application of particle methods to static fracture of reinforced concrete structures. International Journal of Fracture, 2006, 137(1–4): 19–49